Journal of
*Gastroenterology and Hepatology Research*

Online Submissions: http://www.ghrnet.org/index./joghr/
doi: 10.17554/j.issn.2224-3992.2018.07.776

Journal of GHR 2018 August 21; 7(4): 2632-2643
ISSN 2224-3992 (print) ISSN 2224-6509 (online)

ORIGINAL ARTICLE

# Human Hepatic Progenitor Cell Expansion in Liver Fibrosis of Elderly Cadavers

Ki M. Mak, Sophia Chiu

Ki M. Mak, Sophia Chiu, Department of Medical Education and Center for Anatomy and Functional Morphology, Icahn, School of Medicine at Mount Sinai, New York, NY, the United States

Conflict-of-interest statement: The authors declare that there is no conflict of interest regarding the publication of this paper.



Correspondence to: Ki M. Mak, PhD, Icahn School of Medicine at Mount Sinai, Department of Medical Education and Center for Anatomy and Functional Morphology, One Gustave L. Levy Place, Box 1007, New York, NY, the United States.
Email: ki.mak@mssm.edu
Telephone: +1-212 241-7266
Fax: +1- 212 860-1174

Received: May 7, 2018
Revised: June 12, 2018
Accepted: June 15, 2018
Published online: August 21, 2018

## ABSTRACT

**AIMS:** Expansion of human hepatic progenitor cells (HPCs) is a key feature of liver fibrosis associated with a variety of chronic liver diseases. We studied HPC expansion and its relationship to canals of Hering (CoH) and ductular reaction (DR) in liver fibrosis progression of aged cadavers.

**METHODS:** Thirty-five cadavers (83.8 ± 10.8 years) with minimal fibrosis, septal fibrosis, bridging fibrosis and incomplete cirrhosis were studied. Cytokertin 7 immunoperoxidase staining was used to highlight HPCs, CoH and DR.

**RESULTS:** HPC counts in the periportal HPC compartment and in the mid-lobule and centrilobule were 2.3-2.7 times and 2.8-4.5 times higher in advanced fibrosis stages (septal fibrosis, bridging fibrosis and incomplete cirrhosis) compared to minimal fibrosis, respectively. Periportal CoH numbers and DR grades were 2.0-2.6 times and 2.6-2.7 times higher in advanced fibrosis than in minimal fibrosis, respectively. Both CoH numbers and DR grades significantly correlated with periportal HPC counts. There was also a significant correlation between CoH numbers and DR grades. Portal inflammation, but not lobular inflammation, was significant in bridging fibrosis. Steatosis was not an obvious feature associated with the HPC expansion.

**CONCLUSION:** Increased periportal and lobular HPC counts reflect an expansion of HPCs with increased periportal to lobular HPC migration. The expansion likely represents a regenerative response to chronic liver injury in the elderly. Our findings also point to an intricate linkage between the HPCs, CoH and DR in hepatic fibrogenesis. Cadaveric livers provide a source of specimens for evaluating the role of HPCs in fibrosis progression of the aged liver.

**Key words**: Hepatic progenitor cells; Canals of Hering; Ductular reaction; Elderly cadavers; Liver fibrosis progression; Cytokeratin 7 immunoperoxidase



Mak KM, Chiu S. Human Hepatic Progenitor Cell Expansion in Liver Fibrosis of Elderly Cadavers. *Journal of Gastroenterology and Hepatology Research* 2018; **7(4)**: 2632-2643 Available from: URL: http://www.ghrnet.org/index.php/joghr/article/view/2332

## INTRODUCTION

The canals of Hering (CoH) represent the smallest terminal branches of the biliary tree system[1-3]. The canals connect the intrahepatic canalicular channels to the bile ducts in the portal tract. They are specifically located at the interface between the portal tract and periportal parenchyma of the liver lobule. In normal human liver, hepatic progenitor cells (HPCs) reside in a quiescent state in the CoH. When the liver is subjected to acute on chronic injury, HPCs in the CoH become activated, undergoing proliferation and differentiation[4,5,6]. Being bipotential progenitors, HPCs can differentiate into cholangiocytes and hepatocytes. The activation of HPCs is generally associated with a ductular reaction (DR), defined

as a reactive reaction made up of a collection of HPCs around the circumference of the portal tract[7]. These are seen as ductules with no apparent lumen, cell aggregates and solitary single cells embedded in a niche of extracellular matrix and sometime inflammatory cells. This process occurs in the parenchyma of the periportal third of the liver lobule, which has been named the HPC compartment[8-10]. Moreover, depending on the severity of the liver damage, there is a concomitant extension-or migration-of HPCs from the periportal HPC compartment deep into the lobular parenchyma[11].

In human liver disease, DR is closely associated with the severity of fibrosis. The association has been demonstrated in a variety of liver pathologies, including chronic hepatitis C[12], nonalcoholic fatty liver disease with steatohepatitis (NAFLD/NASH)[9,10,13], and alcoholic fatty liver disease[14]. These findings implicate that HPC activation with concurrent DR is a universal phenomenon in response to liver injury regardless of disease etiologies.

Hepatic fibrosis is prevalent in elderly cadavers with diverse causes of death[15]. The fibrosis includes central vein fibrosis, perisinusoidal fibrosis, portal tract fibrosis, septal fibrosis with septa formation, bridging fibrosis with linking septa, incomplete cirrhosis and cirrhosis. Variable degrees of inflammation and steatosis accompany these fibrotic changes. For these reasons, the liver of aged cadavers offers an opportunity to investigate into HPC expansion in association with fibrosis progression. The present study examined the lobular distribution of HPCs and their histological features in the aged cadaveric liver. We then determined the expansion of HPCs in the periportal compartment and extension of HPCs from the peiportal parenchyma into the liver lobule. Correlations between the HPC expansion and CoH and DR were evaluated. Portal inflammation, lobular inflammation and steatosis that may contribute to the HPC expansion were also assessed.

## MATERIALS AND METHODS

### Specimens

Liver tissue of embalmed cadavers from our previous studies provided the source of specimens in the present investigation[15,16]. These liver samples were obtained from cadavers at the end of the Gross Anatomy course at the Icahn School of Medicine at Mount Sinai when the organs were no longer needed. The tissue (~ 1 × 1 × 0.5 cm in size) was excised from the right lobe, placed in formalin and processed for paraffin embedment. The specimens were de-identified so that they could not be linked to the particular subjects. Permission to collect cadaveric livers was granted by the Administrative Manager of Laboratories and Facilities, Department of Medical Education and was approved by the office of Institutional Grants and Contracts. As previously reported[15], these cadaveric livers presented variable tissue preservation (good, fair or poor), evaluated by hematoxylin and eosin (H & E) staining. Based on combined fibrotic changes and tissue preservation (good and at least fair), we selected 35 liver samples (mean age, 83.8 ± 10.8 years) for the present investigation with their demographics summarized in Table 1. These included 10 livers with minimal fibrosis, 10 with septal fibrosis, 10 with bridging fibrosis, and five cases of incomplete cirrhosis (sometimes designated as precirrhosis). The criteria for fibrosis staging based on Sirius red staining of collagens in paraffin-embedded liver sections are presented below. The size of liver sections was ~ 1 × 1 cm, which was sufficiently large to present at least 10 well-defined liver lobules that were demarcated by a central vein in the center with 3 or more portal tracts at the periphery.

**Table 1** Demographic characteristics of cadavers according to the stage of fibrosis.

| Specimen | Age/Gender | Cause of Death |
|---|---|---|
| **Minimal fibrosis** | | |
| 1 | 68F | Cardiopulmonary arrest |
| 2 | 91M | N/A |
| 3 | 74M | N/A |
| 4 | 93M | N/A |
| 5 | 57M | N/A |
| 6 | 91M | Cardiopulmonary arrest, Alzheimer's |
| 7 | 86F | Cerebellar hemorrhage |
| 8 | 74M | Respiratory failure |
| 9 | 92M | Metastatic cancer of unknown origin |
| 10 | 66F | Metastatic lung cancer |
| Mean age = 78.2 ± 12.4 years. | | |
| | | |
| **Septal fibrosis** | | |
| 1 | 75M | N/A |
| 2 | 78F | Cardiac arrest |
| 3 | 81F | N/A |
| 4 | 97M | Congestive heart failure |
| 5 | 98F | Congestive heart failure, hypertensive heart disease |
| 6 | 78F | Cardiopulmonary arrest, emphysema, arteriosclerotic heart disease |
| 7 | 74M | Left lower pneumonia |
| 8 | 98M | Arteriosclerotic heart disease |
| 9 | 99F | Cardiopulmonary arrest |
| 10 | 95M | N/A |
| Mean age = 87.3 ± 10.8 years. | | |
| | | |
| **Bridging fibrosis** | | |
| 1 | 91F | Parkinson's |
| 2 | 85F | Pneumonia |
| 3 | 85M | Cardiovascular disease |
| 4 | 88F | Arrhythmia |
| 5 | 86F | N/A |
| 6 | 81F | Pneumonia |
| 7 | 67M | Kidney cancer |
| 8 | 68M | N/A |
| 9 | 94M | N/A |
| 10 | 92F | B cell lymphoma |
| Mean age = 83.7 ± 9.4 years. | | |
| | | |
| **Incomplete cirrhosis** | | |
| 1 | 90M | Cardiopulmonary arrest |
| 2 | 86M | N/A |
| 3 | 100F | N/A |
| 4 | 85F | N/A |
| 5 | 81F | Respiratory ailure, pulmonary embolus, venous thrombosis |
| Mean age = 88.4 ± 7.2 years. | | |

### Hepatic fibrosis staging

**Minimal fibrosis:** with or without central vein fibrosis; variable perisinusoidal fibrosis; no evidence of portal tract fibrosis.

**Septal fibrosis:** portal tract fibrosis with developing septa from the portal tract; or central vein fibrosis with developing septa from the

vein; variable perisinusoidal/pericellular fibrosis.

**Bridging fibrosis:** portal tract fibrosis with portal-portal linking septum, portal-central linking septum or central-central linking septum; variable perisinusoidal/pericellular fibrosis; no evidence of nodule-like formation.

**Incomplete cirrhosis:** an advanced stage of bridging fibrosis with development of incomplete nodules or nodule-like parenchyma.

**Immunohistochemistry**

Paraffin-embedded liver sections (5-μm in thickness) were simultaneously deparaffinized, rehydrated and antigen unmasked using Trilogy™ solution (a EDTA-based solution, Cell Marque, Rocklin, CA) heated to sub-boiling temperature for 30 min in a kitchen-type steamer, followed by rinsing in another hot bath of Trilogy for an additional 30 min[16]. After cooling, the slides were washed three times in distilled water and then phosphate-buffered saline (PBS). Liver sections were sequentially incubated with peroxide block (10 min), nonspecific protein block (10 min) and antibody to rabbit monoclonal CK7 (1:3000 in 1% bovine serum albumin/PBS; Abcam, Cambridge, MA) for 90 min at room temperature. The immunoreaction was detected with rabbit polymer-HRP (Dako Envision+System, Carpinteria, CA), with buffer washes in between steps. Diaminobenzidine tetrahydrochloride was used as a chromogen to yield a brown color reaction product. Sections were counterstained with Harris hematoxylin for nuclei followed with Sirius red stain for collagens. The specific immunoreactivity of CK7 was verified by positive staining of biliary ducts/ductules in the portal tract, serving as a positive control. Sections that were not antigen retrieved with Trilogy showed negligible or undetectable CK7 immunoreaction.

**Hepatic progenitor cells**

HPCs were positively identified by immunostaining for CK7, as validated (9-12, 17-24). Portal tracts cut transversely or obliquely showing a portal venule and at least one hepatic arteriole and one intraportal biliary ductule were selected for the assessment. $CK7^+$ cells were counted manually under a microscope with 40X and/or 60X objectives. Intermediate hepatocyte-like (IMHL) cells were not included (*infra vide*). Epithelial cells lining the intraportal bile ducts and ductules were not counted. To assess the extension of HPCs from the periportal parenchyma into the lobular area, we scored isolated ductules, cells in aggregates and solitary cells in the mid-lobule - at a distance of ~ 200 μm from the portal tract - and in the centrilobule around the central vein. In each liver section, 10 HPC compartments associated with 10 portal tracts and 10 lobular fields outside the periportal area were assessed. In each fibrosis stage, a total 100 HPC compartments/portal tracts and 100 lobular fields was analyzed, while in the case of incomplete cirrhosis, 50 HPC compartments and 50 lobular fields were assessed. Results were presented as HPC compartment (number of cells per portal tract), and as the number of HPCs per microscopic field in the case of the mid-lobule and centrilobule.

**Canals of Hering**

CoH were identified showing a string of $CK7^+$ epithelial cells, flattened or cuboidal in shape, that emerged from the portal tract perpendicularly or obliquely to the border (limiting plate) of the tract. In most histological sections, CoH were seen to contain about 10 cells in length, ~ 80 μm. As above, portal tracts in cross-sections or oblique sections showing a portal venule and at least one hepatic arteriole and one intraportal biliary ductule were selected for counting the CoH. In each liver, five portal tracts were selected. In total, 50 portal tracts in each fibrosis stage were analyzed, while 25 portal tracts in the liver with incomplete cirrhosis were assessed. Results were expressed as the mean number of CoH per portal tract.

**Ductular reaction**

DR reflected a collection of HPCs around the circumference of a portal tract that included cell aggregates, solitary single cells and ductules. DR was assessed by grading the distribution of these structures relative to the circumference of the portal tracts similar to the schemes of others[17-19]. We graded ductular reaction on a scale of 0, 1, 2 or 3, where 0 indicated absence of $CK7^+$ cells along the border of a portal tract; 1 indicated focal presence of $CK7^+$ cells around the circumference of a portal tract; 2 indicated presence of $CK7^+$ cells occupying less than half of the circumference of a portal tract; and 3 indicted presence of $CK7^+$ cells occupying greater than half of the circumference of a portal tract. In each liver, five portal tracts were taken for the grading, totaling 50 portal tracts in each fibrosis stage. In the liver with incomplete cirrhosis, 25 portal tracts were analyzed. The grading was presented as the mean grade per portal tract.

**Portal and lobular inflammation**

Portal inflammation was recognized as presence of small round cells in the stroma of portal tracts on H&E sections. Score 0 indicated sporadic presence of inflammatory cells; score 1 indicated diffuse presence of inflammatory cells in the portal stroma; score 2 indicated aggregates of inflammatory cells occupying less than half of the portal stroma; and score 3 indicated aggregates of inflammatory cells occupying more than half of the portal stroma. In each liver, scoring was based on the most severely affected portal tracts. Lobular inflammation was scored as follows: 1 indicated scattered and isolated mononuclear and/or polymorphonuclear leucocytes in the sinusoidal lumens; 2 indicated diffused presence of inflammatory cells in the sinusoidal lumens. When inflammatory cells were detected in the liver lobular parenchyma, an additional score of 1 was added, making a score of 2 or 3.

**Steatosis**

Steatosis was assessed on H&E sections. Steatosis was scored 1-3 based on the proportion of the liver lobule occupied by fatty hepatocytes - containing macrovesicular or microvesicular droplets or both: 1 = 1/3 of the liver lobule, generally centrilobular location; 2 = 2/3 of the liver lobule, generally centrilobular-midlobular location; and 3 = panlobular.

**Statistics**

Data were reported as means ± SEM. Statistical significance was determined by Student's t-tests. The correlations between two parameters were evaluated by the Pearson coefficient correlations. $P < 0.05$ was considered statistically significant. Statistics were performed using Microsoft™ Excel™ for Mac 2011, version 14.50.

## RESULTS

The demographics of the 35 cadavers are summarized in Table 1. There was no significant difference in the age between groups. As a whole, the mean age was 83.8 ± 10.8 years (range 57-100 years; N = 35). Eighteen were male and 17 female. Of the males, 6 were less than 84 years old and 12 more than 84 years. Of the females, 7 were less than 84 years old and 10 were more than 84 years. Causes of death were available in 22 donors: 15 were pulmonary, cardiac

and vascular-related with or without additional diseases, 4 were cancer-related, 1 had cerebellar hemorrhage and one had Parkinson's disease. No liver disease was indicated as the cause of death in these 22 donors; however, this did not exclude that they had ongoing liver disease. Moreover, it is not known if liver disease was indicated among the 13 donors with no causes of death available.

**Survey of lobular distribution of CK7 immunostaining**

We first surveyed the distribution of CK7 immunostaining in the cadaveric livers (Figure 1). In the liver with little fibrotic changes, CK7 staining was generally absent, barely discernable, or visible in the periportal compartment around the portal tract. CK7 staining was inconspicuous or sparingly present in the lobular parenchyma outside the periportal area. In comparison, in the liver with more or severe fibrotic changes, $CK7^+$ cells were quite obvious in the periportal compartment. There were clusters of variable sizes of $CK7^+$ cells as well as solitary single $CK7^+$ cells that were readily discernable in the lobular parenchyma outside the periportal area.

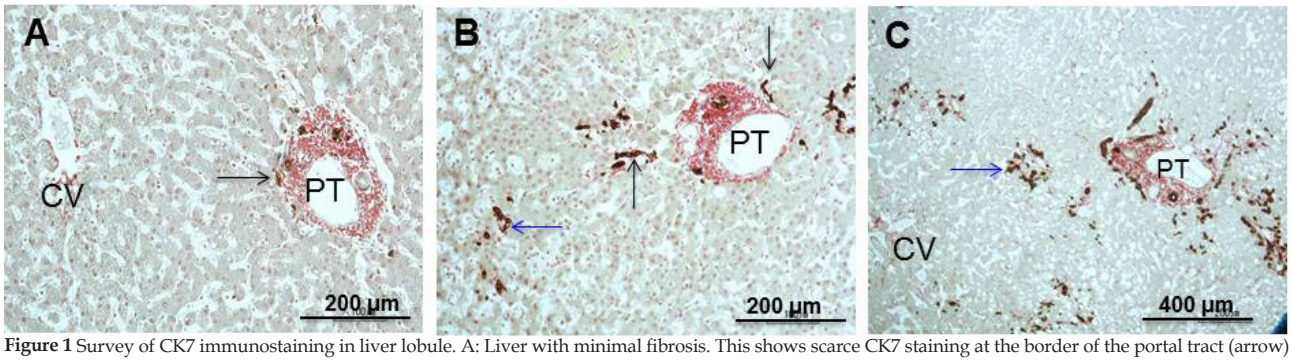


**Figure 1** Survey of CK7 immunostaining in liver lobule. A: Liver with minimal fibrosis. This shows scarce CK7 staining at the border of the portal tract (arrow) and undetectable CK7 staining in the lobular parenchyma. B: Liver with septal fibrosis. CK7 staining reaction is evident in the periportal parenchyma (black arrow) and in the mid-lobule (blue arrow). C: Liver with septal fibrosis. Marked CK7 staining around the portal tract and in the mid-lobule (blue arrow) is seen. Note that in all cases intraportal ductules are stained for CK7. Sirius red post-stained. PT, portal tract; CV, central vein.

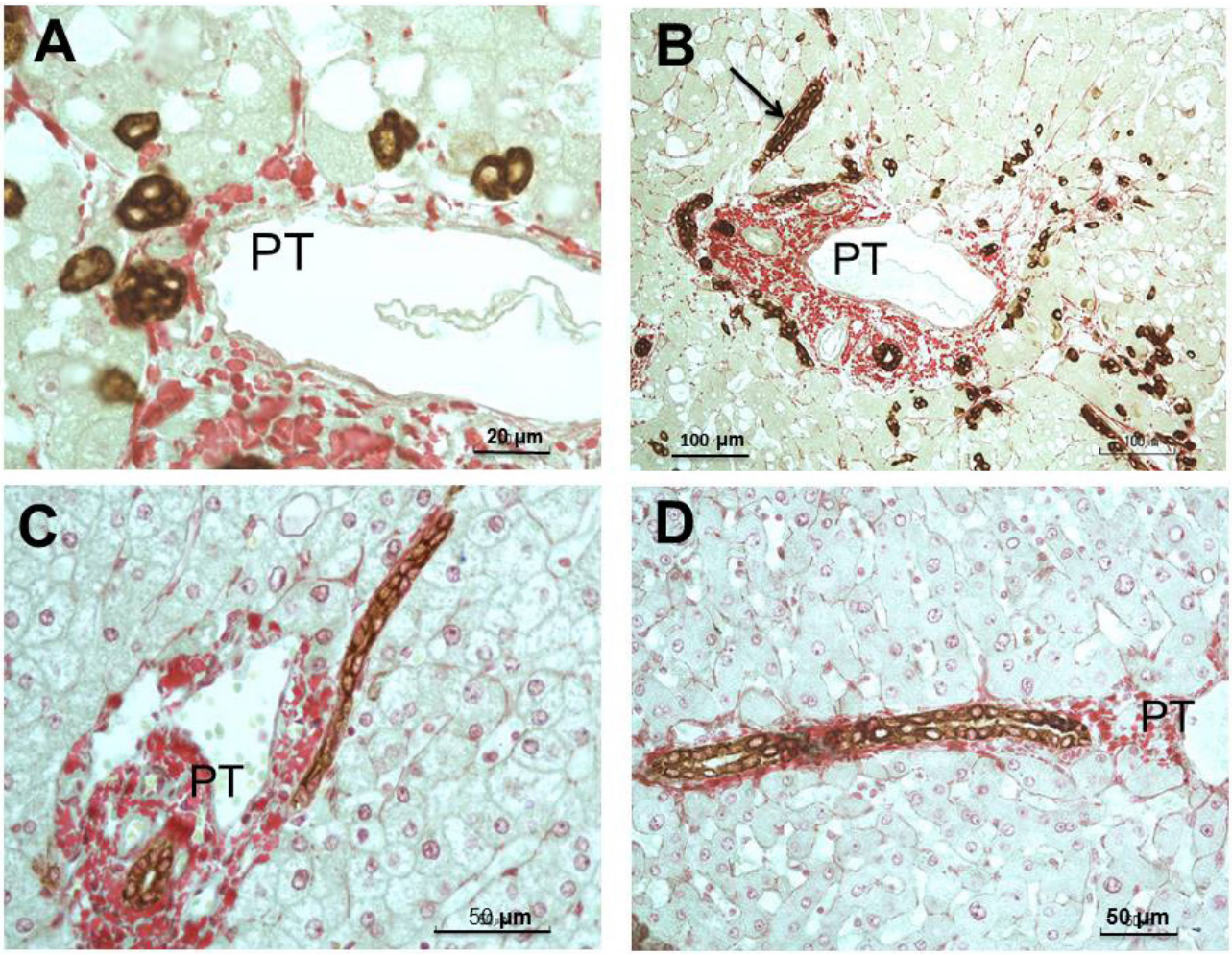


**Figure 2** Histological features of CK7-immunostained HPCs in the periportal HPC compartment. A: CK7+ HPCs in the form of clumps, triplet, doublet and singly at the border of the portal tract. The HPCs are ovoid-shaped (~ 8 μm in size) containing an ovoid nucleus and a thin rim of cytoplasm strongly stained for CK7. B: The arrow marks a canal of Hering—sectioned somewhat obliquely and measured ~ 150 μm long—in the vicinity of the periportal parenchyma. It appears to contain two strands of flattened cells strongly stained for CK7. There are also CK7 stained structures in the form of twisted strings of varied sizes, aggregates of cells and single cells in the periportal parenchyma. C: This shows a canal of Hering as it emerges from the portal tract into the periportal parenchyma. D: A canal of Hering sectioned lengthwise. The lining cells, vividly stained for CK7, are squamous-cuboidal shaped and enclose a narrow lumen. It is ~ 300 μm in length, which is nearly the width of the periportal third of a liver lobule. Sirius red post-stained. PT: portal tract.

Next, we examined the histological features and arrangement of CK7$^+$ HPCs. HPCs were small oval- or cuboidal-shaped cells (~ 8 μm in size) showing an ovoid nucleus and scant cytoplasm that was vividly stained for CK7, in concordance with the use of CK7 as a phenotypic marker of HPCs in chronic liver diseases[9-12,17-24]. In other studies, CK19 and EpCAM (epithelial cell adhesion molecule) have also been used[17,25,26]. In the periportal HPC compartment, CK7$^+$ cells were disposed in strings/cords - tightly twisted - without a discernable lumen. They also presented in small clumps, triplets and doublets, as well as singly along the border of the portal tract (Figure 2A). At this location, CK7$^+$ cells were also observed to line the CoH that revealed a narrow lumen depending on the plane of sectioning (Figure 2B and C). In rare occasions, one could see a canal as long as 300 μm, nearly traversing the entire width of the periportal third of the lobule (Figure 2 D). Figure 3 A-E illustrate the diverse histological features and disposition of CK7$^+$ cells in the mid-lobular parenchyma. In a number of livers with advanced stages of fibrosis, we could see CK7$^+$ cells aggregated with IMHL cells; the latter were identified by a distinct cell membrane and faint cytoplasmic immunostaining for CK7 (Figure 3 F and G). These cells were not included in the counting of HPCs - as indicated in the Method section. It was common to locate CK7$^+$ cells in foci of marked perisinusoidal/pericellular fibrosis (Figure 4 A-C). CK7$^+$cells were often found at the septal-parenchymal borders of developing septa and bridging septa (Figure 4D).

**Quantification of HPCs in progressive fibrosis**

Having defined the lobular distribution of CK7$^+$ cells and their histological features, we quantified the CK7$^+$ cells according to the stage of fibrosis (Figure 5). The number of cells in the periportal HPC compartment increased from 8.14 ± 1.44 per portal tract in minimal fibrosis to 18.91 ± 3.04 in septal fibrosis ($P < 0.01$), 21.81 ± 4.10 in bridging fibrosis ($P < 0.01$), and 17.92 ± 2.18 in incomplete cirrhosis ($P < 0.01$). In the mid-lobule and occasionally the centrilobule, the HPC count was 2.57 ± 1.11 cells/field in minimal fibrosis. The number rose to 7.08 ± 1.54 cells/field in septal fibrosis ($P < 0.05$), 11.59 ± 2.18 cells/field in bridging fibrosis ($P < 0.001$), and 9.62 ± 0.65 in incomplete cirrhosis ($P < 0.001$). We also estimated that 24% of HPCs was distributed outside the periportal HPC compartment in minimum fibrosis, 27% in septal fibrosis and 35% in bridging fibrosis, and 40% in incomplete cirrhosis. These data demonstrate a striking expansion of HPCs with a 2.2-2.6 times increase of HPCs in the periportal HPC

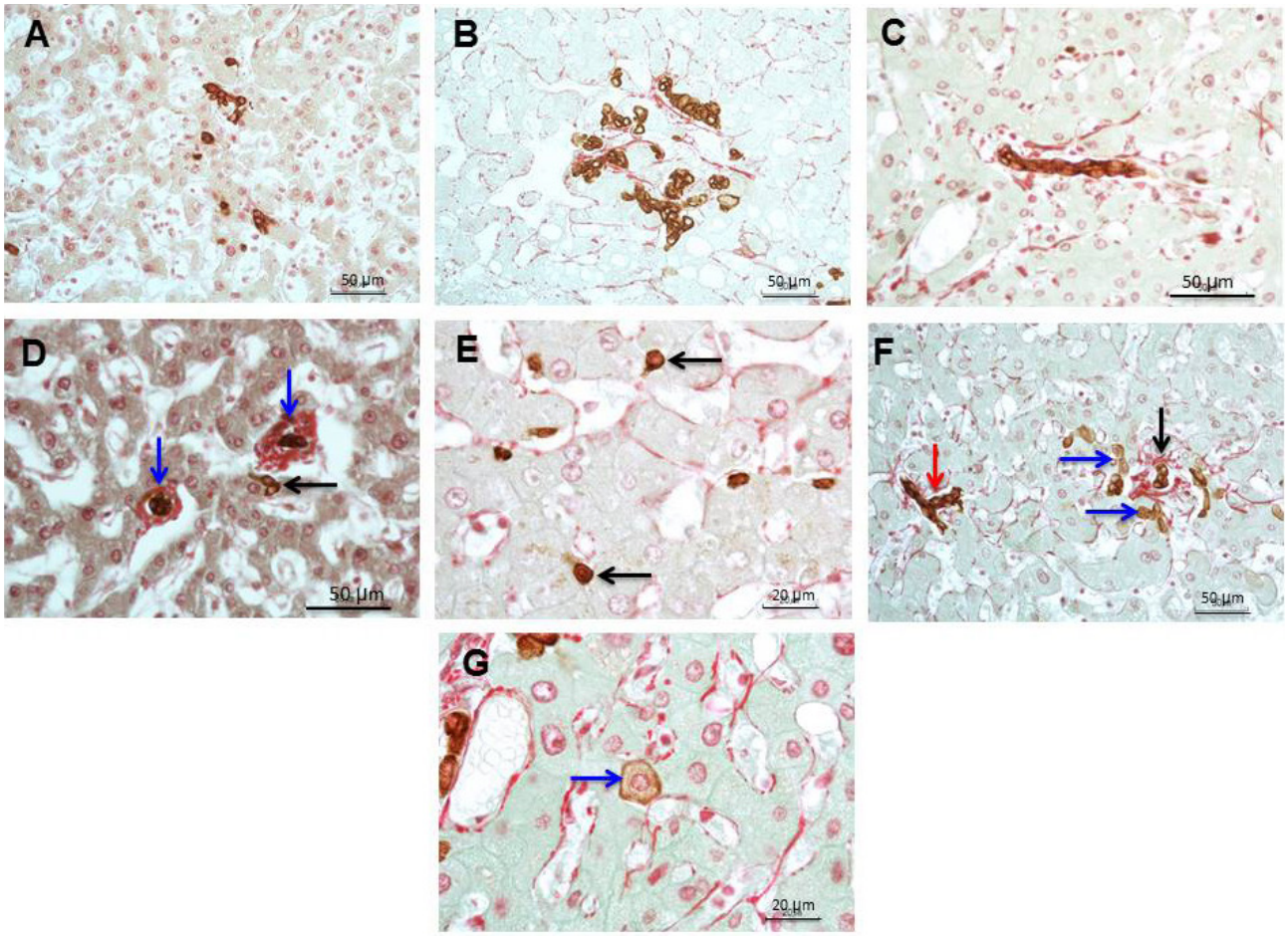


**Figure 3** Histological features of HPCs in mid-lobule. A: Small aggregates of CK7+ cells and a few solitary single cells in the lobular parenchyma. B: A large aggregate (~180 μm in size) of CK7+ cells in the lobular parenchyma. Cells appear tightly twisted, in small clumps or solitary. C: An isolated cord/string of CK7+ cells. It is composed of two strands of flattened cells, intertwined and without an apparent lumen. It appears to situate between the liver plates rather than in the sinusoid. D: CK7+ cells in an aggregate of three and four cells ensheathed by a thick band of collagenous matrix stained red with Sirius red stain (blue arrows). Note two individual CK7+ cells that are not surrounded by a collagenous matirx (black arrow); these are more vividly illustrated in image E: Solitary single HPCs. These are small oval-shaped cells ( ~ 8 μm in size) containing a thin rim of cytoplasm strongly stained for CK7; two of them are marked by arrows. They are located in the space of Disse or between the hepatocytes and are not surrounded by a collagenous matrix. F: In the mid-lobule of some liver specimens with severe fibrotic changes, one could see a collection of small oval-shaped CK7+ cells (black arrow) and cells that exhibit features of IMHL cells (blue arrows). Note a string of CK7+ cells are seen nearby (red arrow). G: The arrow indicates an IMHL cell, which is polygonal in shape and is smaller than the hepatocyte but larger than the HPC. It displays a distinct staining of the cell membrane and a faint staining of the cytoplasm for CK7. IMHL cell is not surrounded by a collagenous matrix. Sirius red post-stained.

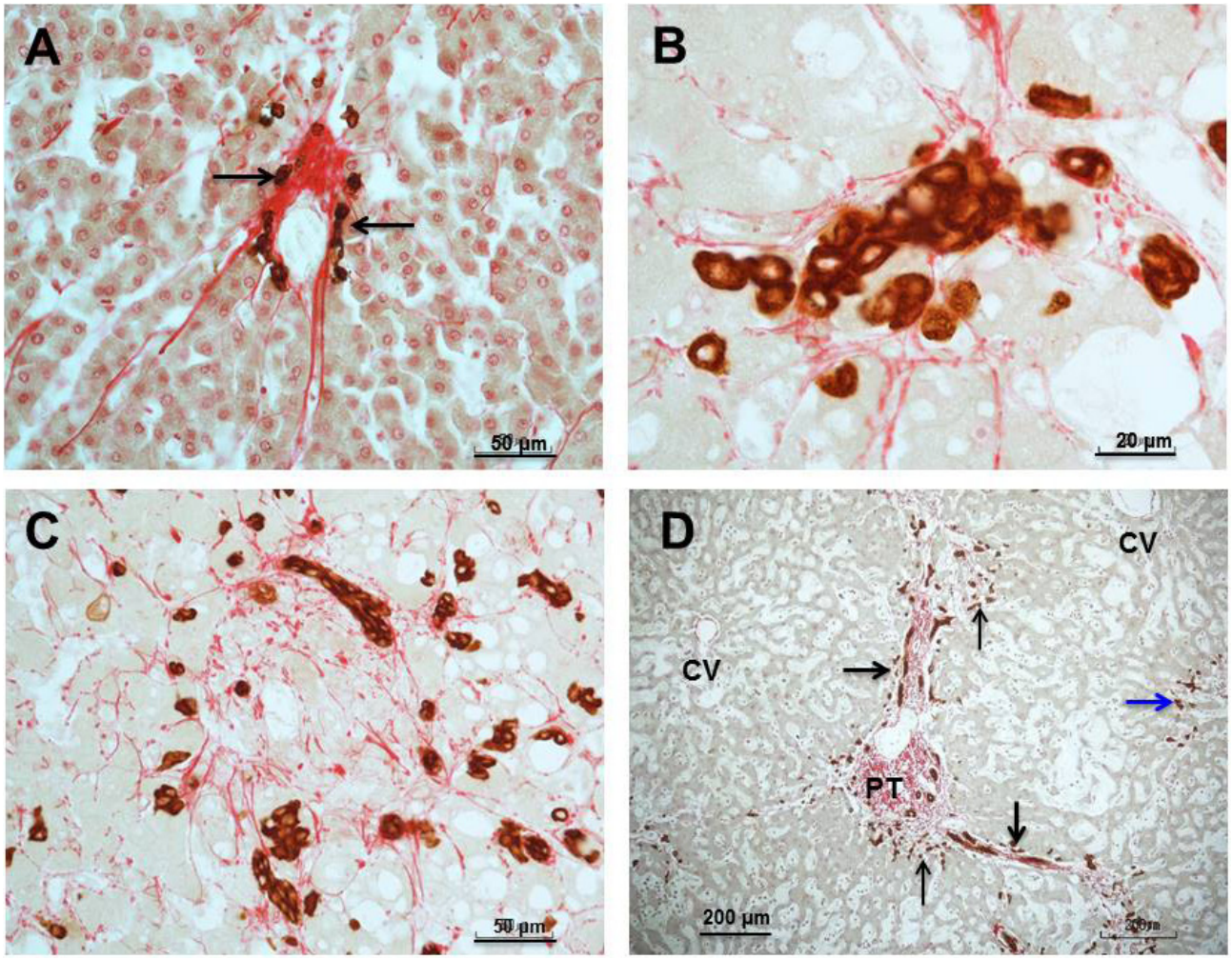


**Figure 4** A-C: Localization of HPCs in foci of parenchymal fibrosis. A: CK7+ cells in single or strands (arrows) in close association with a small fibrotic lesion (~ 60 μm) stained red with Sirius red. B: CK7+ cells in a tightly packed clump in a small fibrotic lesion (~ 80 μm). Individual CK7+ cells are also present. C: CK7+ cells in a relative large lesion (~150 μm across) of marked perisinusoidal fibrosis. The cells appear as strands of two rows of flattened cells, resembling a ductule or canal, and clumps as well as solitary single cells. D: A portal tract with two developing septa extending from the tract. CK7+ cells are seen disposed along the septal-parenchymal borders and at the growing front of the septa (arrows). The blue arrow marks an aggregate of CK7+ cells in the mid-lobular parenchyma. Sirius red post-stained. CV: central vein, PT: portal tract.

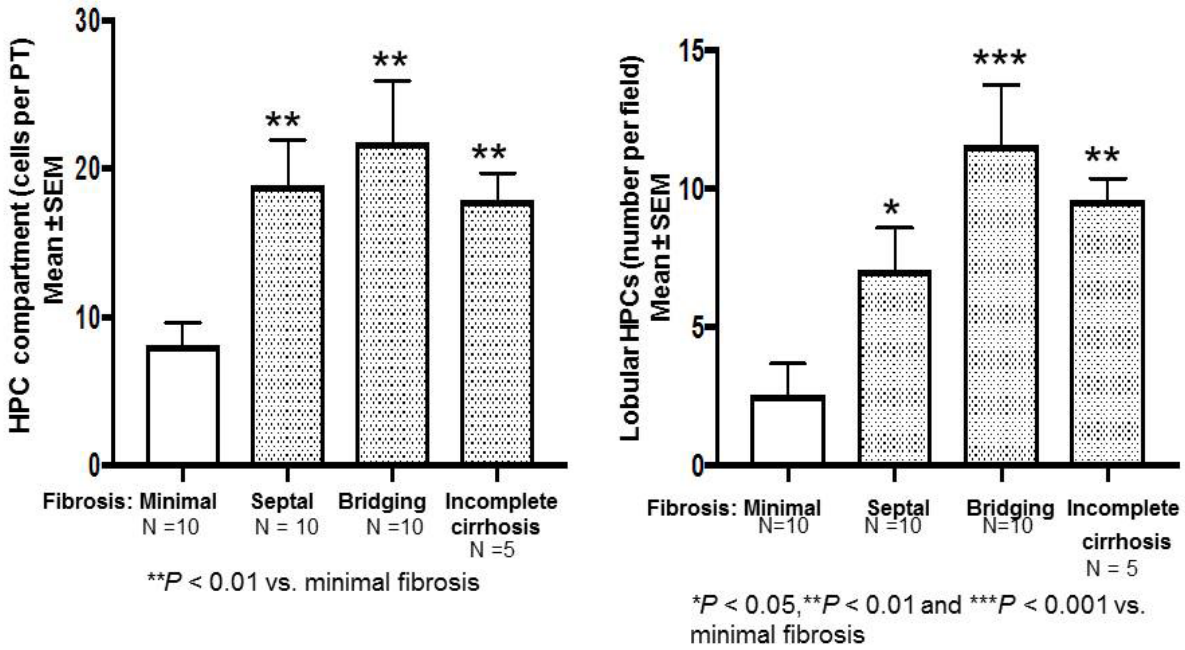


**Figure 5** Quantification of HPCs in periportal HPC compartment and in lobular parenchyma. A: HPC counts in the HPC compartment. B: HPC counts in the lobular parenchyma distal to the periportal area. In both areas, HPC numbers are significantly greater in the liver with septal fibrosis, bridging fibrosis and incomplete cirrhosis than in the liver with minimal fibrosis. PT: portal tract.

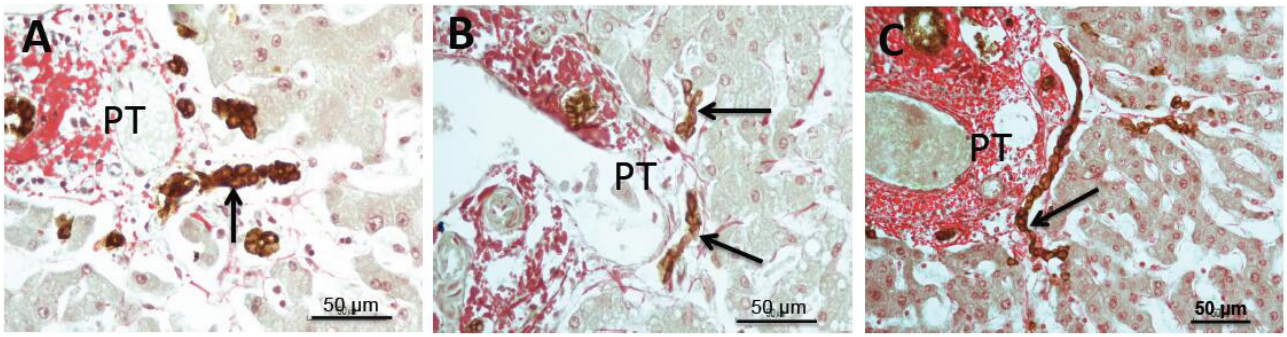


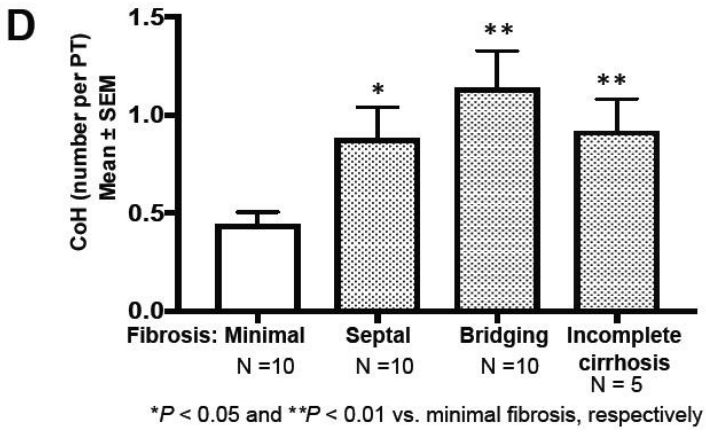


**Figure 6** A-C: Representative images illustrating the disposition of CoH as they emerge from the portal tract into the periportal parenchyma through the limiting plate. At this location, the canals (arrows) appear perpendicularly or obliquely to the border of the portal tract. The cells are strongly CK7 positive. They are generally 5-10 cell long, ~ 30 - 80 μm in length. They are arranged in two cell layers, somewhat twisted with a hardly discernable lumen. In image C, it is evident that the canal is in continuation with the intraportal bile ductule (at arrow). Sirius red post-stained PT, portal tract. D: CoH counts in periportal compartment according to fibrosis stages. CoH numbers are significantly greater in the stages of septal fibrosis, bridging fibrosis and cirrhosis compared to minimal fibrosis. PT: portal tract.

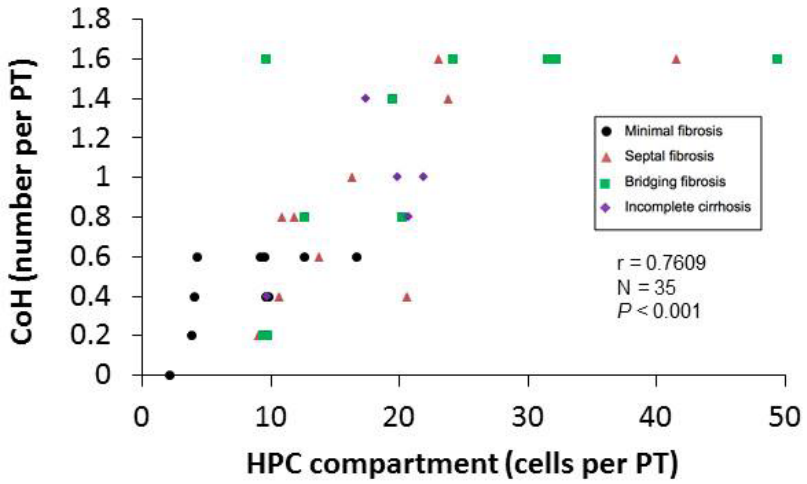


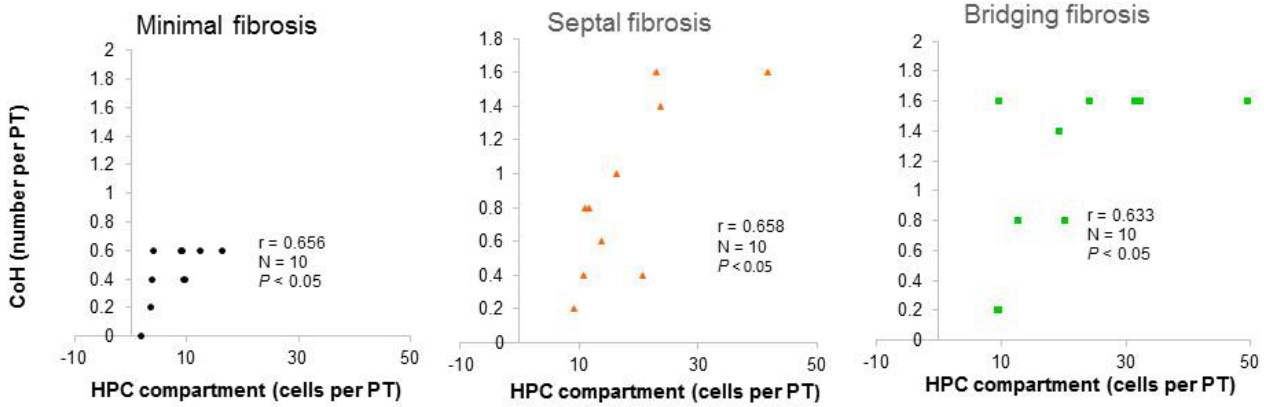


**Figure 7** Relationship between the number of CoH and expansion of HPC compartment according to the stage of fibrosis. **Upper panel:** There is a strong correlation between the number of CoH and the number of HPCs in progressive fibrosis stages. **Lower panel:** In each stage - minimal fibrosis, septal fibrosis and bridging fibrosis - the number of CoH is correlated with the number of HPCs. Note that the data from incomplete cirrhosis (N = 5) were not included in the analysis. PT: portal tract.

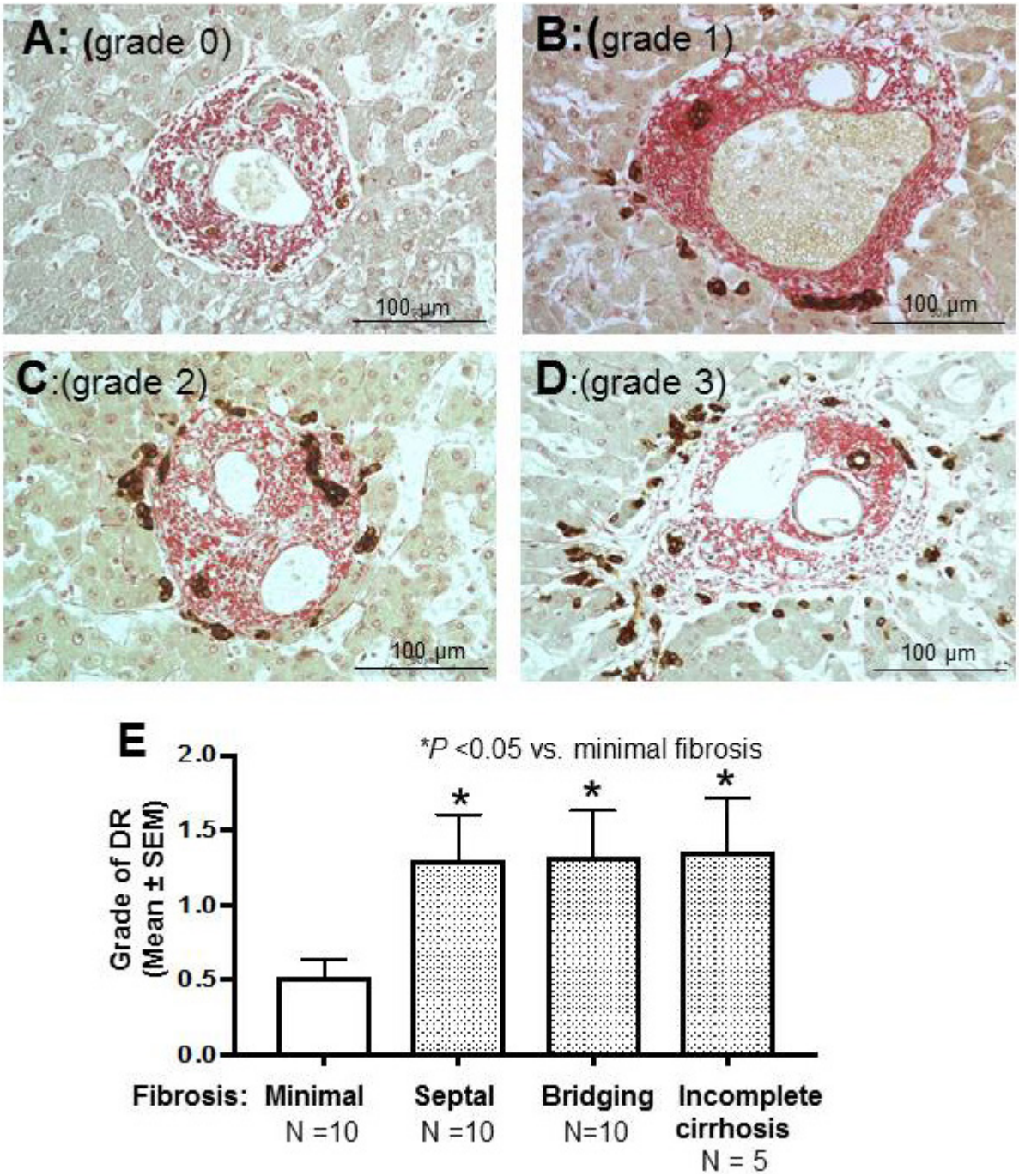


**Figure 8** Representative images illustrating the morphological grading of DR based on CK7 immunoperoxidase staining. A: Grade 0, B: Grade 1, C: Grade 2, and D: Grade 3. See grading criteria in the METHOD section. Note that CK7 stained ductules in the portal tract stroma are not included in the grading. Sirius red post-stained. E: Assessment of the extent of DR based on DR grades. DR grades in septal fibrosis, bridging fibrosis and incomplete cirrhosis are significantly higher than the DR grade in minimal fibrosis.

compartment and a 2.8-4.5 times increase of HPCs in the mid-lobular parenchyma as fibrosis progresses from minimal fibrosis to advanced stages of fibrosis. The higher HPC counts in the lobule distal to the periportal parenchyma likely resulted from portal to lobular migration of HPCs, in concordance with the observation of a previous study in patients with chronic hepatitis B and C[10].

**Correlation between CoH and HPCs in liver fibrosis**

To determine whether there is a relationship between the incidence of CoH and HPC numbers in the periportal compartment, the number of CoH was counted. We first illustrated the histological features of CoH highlighted by CK7 immunostaining of HPCs (Figure 6A), and then presented the counts of CoH according to the stages of fibrosis (Figure 6B). CoH numbers increased from 0.44 ± 0.07 per portal tract in minimal fibrosis to 0.88 ± 0.16 ($P < 0.05$) in septal fibrosis, to 1.14 ± 0.16 ($P < 0.01$) in bridging fibrosis, and to 0.92 ± 0.11 ($P < 0.01$) in incomplete cirrhosis. Thus, the incidence of CoH in advanced fibrosis stages was 2.0-2.6 times higher than in the minimal fibrosis. When CoH numbers were plotted against HPC numbers in the HPC compartment, a strong correlation between these two parameters was found, $P < 0.001$, N =35 (Figure 7A). Furthermore, there was a significant correlation between the numbers of CoH and HPCs according to the fibrosis stage (Figure 7B), thereby linking CoH proliferation to HPC expansion. These data are in accord with the view that the CoH are a potential source of HPCs, observed in patients with chronic hepatitis C, hepatic B and autoimmune hepatitis[17].

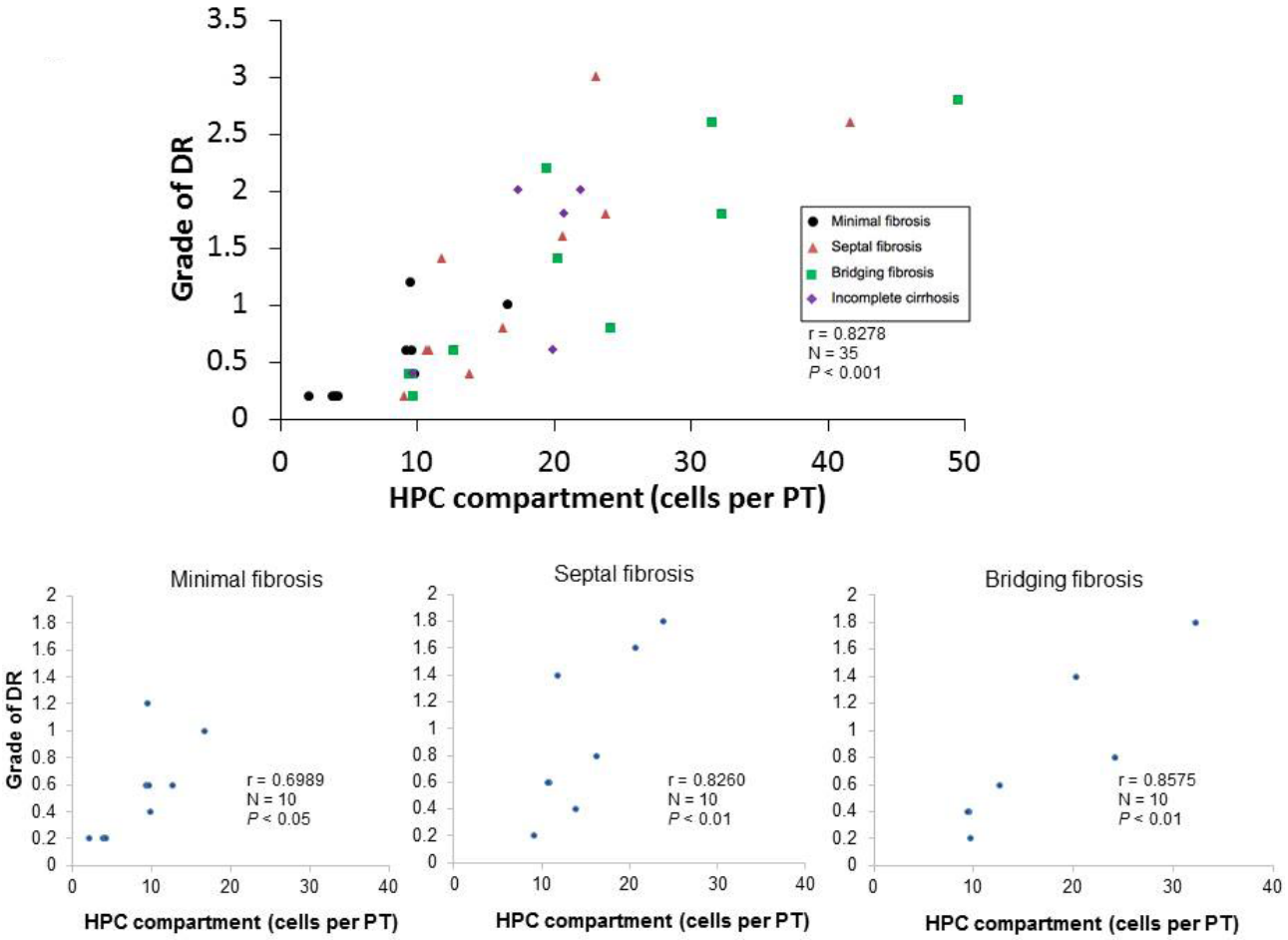


**Figure 9** Relationship between DR extent and expansion of the HPC compartment. **Upper panel:** There is a highly significant correlation between DR grades and HPC numbers in progressive fibrosis stages. **Lower panel:** In each stage - minimal fibrosis, septal fibrosis and bridging fibrosis - the DR grade is correlated with the number of HPCs. Note that the data from incomplete cirrhosis (N = 5) were not included in he analysis. PT: portal tract.

**Correlation between DR grades and HPCs in liver fibrosis**

Since the extent of DR has been shown to be associated with progressive fibrosis in a number of liver diseases[9,12,17], we determined the grades of DR in the liver of aged cadavers. The histological grading of DR is illustrated in Figure 8 A-D, and the DR grades accompanied the stages of fibrosis are presented Figure 8E. The DR grade in minimal fibrosis was 0.50 ± 0.15. DR grades in septal fibrosis (1.30 ± 0.36), bridging fibrosis (1.32 ± 0.30) and incomplete cirrhosis (1.36 ± 0.24) were 2.6-2.7 times higher compared to minimal fibrosis ($P < 0.05$). When DR grades were plotted against HPC numbers in the HPC compartment, a strong correlation between these two variables was found, $P < 0.001$; N = 35 (Figure 9A). Furthermore, the grade of DR was significantly correlated with the number of HPCs according to the fibrosis stage (Figure 9B). These findings point to a link between the extent of DR and expansion of HPCs in liver fibrosis progression.

**Correlation between CoH numbers and DR extent**

Since the periportal HPC population correlated with CoH numbers as well as with DR grades, we predicted a correlation between the CoH and DR as well. Accordingly, Figure 10 demonstrates a strong correlation between the incidence of CoH and extent DR in cadaveric livers with progressive fibrosis ($P < 0.001$). The relationship reveals an anatomical linkage between CoH and DR in hepatic fibrogenesis of the aged cadavers.

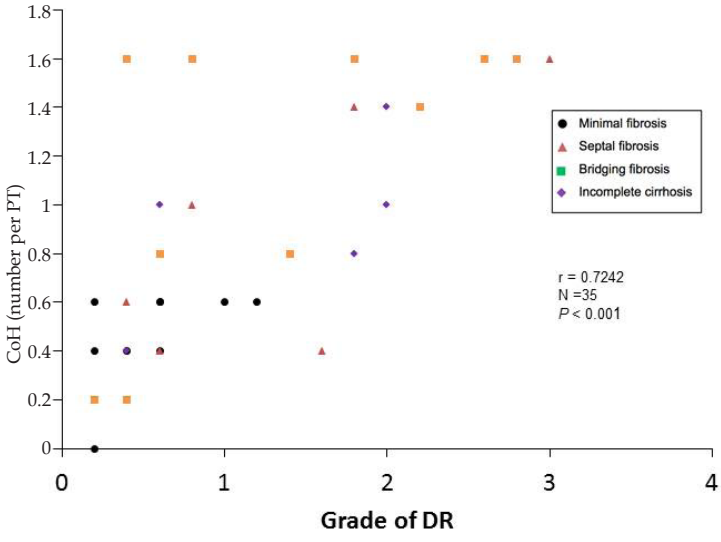


**Figure 10** Relationship between CoH and DR. CoH numbers and DR grades from the liver with minimal fibrosis, septal fibrosis, bridging fibrosis and incomplete cirrhosis are significantly correlated. PT: portal tract.

**Hepatic inflammation and steatosis**

To evaluate whether liver inflammation contributes to the HPC expansion, we determined inflammatory changes accompanying the stages of fibrosis. As summarized in Table 2, the portal tract inflammation score was significantly higher in the bridging fibrosis

than in the minimal fibrosis stage ($P < 0.01$), suggesting that the inflammation contributes to the HPC expansion in the liver with bridging fibrosis. Lobular inflammation invariably occurred in the aged cadavers, and the scores did not differ among the fibrosis stages.

We assessed steatosis in the aged cadavers. Table 3 summarized the incidence of fatty liver and steatosis grades according to the stage of fibrosis. The overall incidence of fatty liver in 35 cadavers was 31.4 %, a level nearly similar to that observed in our previous study, 35.5% in 68 cadavers[15]. However, steatosis was not an obvious feature associated with the stage of fibrosis; cadavers without fatty liver also had HPC expansion.

**Table 2** Inflammation scores in aged cadavers

| Stage of Fibrosis | Portal Inflammation | Lobular Inflammation |
|---|---|---|
| Minimal fibrosis | 1.5 ± 0.22 | 1.8 ± 0.29 |
| Septal fibrosis | 2.0 ± 0.21 | 2.1 ± 0.31 |
| Bridging fibrosis | 2.6 ± 0.20** | 1.9 ± 0.31 |
| Incomplete cirrhosis | 2.0 ± 0.45 | 1.6 ± 0.51 |

**Bridging fibrosis vs. minimal fibrosis, $P < 0.01$.

**Table 3** Steatosis scores in aged cadavers.

| Stage of fibrosis | Steatosis incience | Steatosis grade |
|---|---|---|
| Minimal fibrosis | 3/10 livers | 1, 2, 2 |
| Septal fibrosis | 4/10 livers | 2, 3, 3, 3 |
| Bridging fibrosis | 1/10 livers | 1 |
| Incomplete cirrhosis | 3/5 livers | 1, 2, 2 |

The incidence of steatosis in 35 cadavers is 31.4% and the grades of steatosis varied from 1 to 3.

## DISCUSSION

The present study demonstrates that the HPC population in the periportal HPC compartment markedly expands with a concomitant greater extension of HPCs into the lobule outside the periportal area in the aged liver with septal fibrosis, bridging fibrosis and incomplete cirrhosis compared to minimal fibrosis. The expansion of the HPC compartment correlates with increased CoH numbers and higher DR grades accompanying the fibrosis progression. There is also a significant correlation between the incidence of CoH and grades of DR. Taken together, the findings point to an intricate linkage between HPCs, CoH and DR in hepatic fibrogenesis of the aged cadavers.

Extension - also described as migration - of HPCs from the periportal area centrally into the liver lobule was first described in chronic viral hepatitis B and C with severe parenchymal inflammation[11]. The phenomenon has frequently discussed in association with investigations of fibrotic disease[17,18]. In the cadavers, we estimated that about 25% to 40% of the HPCs were distributed in the lobular parenchyma outside the periportal area of the liver with minimal fibrosis, septal fibrosis, bridging fibrosis and incomplete cirrhosis. HPC counts also showed a 2.8 - 4.5 times increase of HPCs in the lobular parenchyma in progressive fibrosis. The anatomical pathway of periportal to lobular migration of HPCs has not been established. It has been suggested that the HPCs move along the interstitium of the space of Disse[27]. The fate of these migratory HPCs in the hepatic lobules outside the periportal area has not been determined. It is likely that they differentiate into solitary HPCs that are seen in the Disse's space and in the intercellular space of hepatocytes (Figure 4E), as previously described in human chronic liver disease and in experimental liver injury[17,27,28]. At these locations, solitary progenitor cells may transform into IMHL cells that can be highlighted by a distinct CK7 immunostaining of the cell membrane in conjunction with a faint cytoplasmic staining (Figure 4G). The distribution of IMHL cells is possibly related to hepatic regeneration in response to liver injury consequent to fibrosis[13]. This scenario has been described in people with chronic viral hepatitis[11,17,18], alcoholic hepatitis[23] and alcoholic and NAFLD[5,14], and in pediatric NAFLD/NASH[10].

The CoH are residence for HPCs[2,7]. The canals provide a source of progenitor cells that subsequently form ductules, cell aggregates and solitary cells in the periportal HPC compartment, often described as DR (*supra vide*). Our data indicate that the CoH at the interface of the portal tract and periportal parenchyma increase in progressive fibrosis stages from minimal fibrosis to advanced fibrosis. These changes occur in parallel with the rise of $CK7^+$ cell counts in the HPC compartment, thereby linking proliferation of CoH to expansion of the HPC compartment. Furthermore, we found that the number of CoH correlates with the extent of the DR according to the stage of fibrosis, implicating a morphological link between the CoH and DR, which is in concordance with the view proposed by Eleazar *et al*[17].

Assessment of periportal DR has been considered a useful marker in the evaluation of the HPC activation in a variety of chronic liver diseases. An increased DR extent is associated with a HPC expansion in patients with NASH and the extent correlates with the degrees of NASH activity[9]. DR is prominent in the majority of patients with chronic hepatitis C, B and autoimmune hepatitis[17]. In hepatitis C, a strong correlation was noted between the DR and HPC expansion as well as the degrees of portal fibrosis[12]. Moreover, DR was found to occur preceding the onset of portal fibrosis, implicating that the DR initiates the fibrosis. In alcoholic hepatitis, which is an acute-on-chronic condition, DR is a key event and along with the HPC expansion parallels the disease activity[29]. In the aged cadavers, we observed little or no DR in the liver with minimal fibrosis, whereas DR became more evident and conspicuous in septal fibrosis, bridging fibrosis and incomplete cirrhosis. Our data also indicate that the DR grades correlated with HPC counts as well as CoH numbers in the periportal parenchyma according to the fibrosis stage. Thus, these associations implicate a link between periportal DR, HPCs and CoH in liver fibrogenesis, consistent with the studies of others (reviewed in 30).

Inflammatory changes of the aged cadavers are common. Our data showed a trend of increased portal inflammation scores from minimal fibrosis to advanced stages of fibrosis. The inflammation in bridging fibrosis actually is significantly greater than that of minimal fibrosis. The observation appears to be consistent with the study in which portal inflammatory infiltrate is a key feature of NAFLD and can be linked to the extent of DR and HPC expansion in progressive stages of NASH[19]. Similar degrees of lobular inflammation occur in the cadaveric livers and the changes could not be related to the HPC expansion. Concerning steatosis, in patients with chronic hepatitis infection, steatosis was shown to exacerbate the periportal HPC expansion and DR, but the fatty change was not an obligate feature[12]. In the aged cadavers, the incidence of steatosis in 35 livers is 31.4%. Steatosis is not an obvious feature associated with the stage of fibrosis, and the cadavers without fatty liver also has HPC expansion.

The question could be raised of whether aging has any effects on the prevalence of HPCs in the human liver. In this regard, it is worth noting that, in chronic hepatitis C, HPC activation is a common but diverse phenomenon closely related to the patient age and hepatitis stage[18]. It was found that patients older than 40 years have a higher

number of HPCs and CK7 staining of hepatocytes than younger patients. Another study of chronic hepatitis C infected patients reported a correlation of HPC expansion and DR with increasing age[12]. Since our cadavers have a mean age of 83.8 year, it will be interesting to compare the HPC expansion in these aged people with a younger group of cadavers - below 65 years. This awaits future investigation.

In conclusion, increased HPC counts in the periportal HPC compartment along with increased lobular distribution of HPCs outside the periportal area reflect an expansion of HPCs. The positive correlations between HPCs and COH and DR suggest a linkage between these constituents. The expansion likely represents a regenerative response to liver injury caused by fibrosis in the elderly. Because of the diverse causes of death and the lack of information whether there was any ongoing liver disease in these cadavers, we cannot associate the HPC response to any specific liver disease. Nonetheless, our findings implicate that the HPC expansion is a universal phenomenon associated with chronic liver damage regardless of disease etiologies. Cadaveric livers provide a source of specimens for evaluating the role of HPCs in fibrosis progression in the aged liver. Finally, whether aging has any effects on the HPC expansion is a challenging question that awaits future investigation.

## ACKNOWLEDGEMENTS

The authors wish to acknowledge the support by the Research Fund of the Center for Anatomy and Functional Morphology at Icahn School of Medicine at Mount Sinai.

## REFERENCES

1. Saxena R, Theise ND, Crawford JM. Microanatomy of the human liver—Exploring the hidden interfaces. *Hepatology* 1999; **30(6):**1339-1346. [PMID: 10573509]; [DOI: 10.1002/hep510300607]
2. Theise ND, Saxena R, Portmann BC, Thung SN, Yee H, Chiriboga L, Kumar A, Crawford JM. The canals of Hering and hepatic stem cells in humans. *Hepatology* 1999; **30(6):**1425-1433. [PMID: 10573521]; [DOI: 10.1002/hep510300614]
3. Gouw ASH, Clouston AD, Theise ND. Ductular reactions in human liver: Diversity at the interface. *Hepatology* 2011; **54(5):**1853-1863. [PMID: 21983984]; [DOI: 10.1002/hep24613]
4. Sell S. Heterogeneity and plasticity of hepatocyte lineage cells. *Hepatology* 2001; **33(3):** 738-750. [PMID: 11230756]; [DOI: 10.1053/jhep.2001.21900]
5. Roskams TA, Libbrecht L, Desmet VJ. Progenitor cells in diseased human liver. *Sem Liver Dis* 2003; **23(04):** 385-396. [PMID: 14722815]; [DOI: 10.1055/s-2004-815564]
6. Bird TG, Lorenzini S, Forbes SJ. Activation of stem cells in hepatic diseases. *Cell Tissue Res* 2008; **331(1):** 283-300. [PMID: 18046579]; [DOI: 10.1007/s00441-007-0542-z]
7. Roskams TA, Theise ND, Balabaud C, Bhagat G, Bhathal PS, Bioulac-Sage P, Brunt EM, Crawford JM, Crosby HA, Desmet V, Finegold MJ, Geller SA, Gouw ASH, Hytiroglou P, Knisely AS, Kojiro M, Lefkowitch JH, Nakanuma Y, Olynyk JK, Park YN, Portman B, Saxena R, Scheuer PJ, Strain AJ, Thung SN, Wanless IR, West AB. Nomenclature of the finer branches of the biliary tree: canals, ductules, and ductular reactions in human livers. *Hepatology* 2004; **39 (6):** 1739-1745. [PMID: 15185318]; [DOI: 10.1002/hep.20130]
8. Libbrecht L, Roskams T. Hepatic progenitor cells in human liver diseases. *Sem Cell Develop Biol* 2002; **13(6):** 389-396. [PMID: 12468238]; [DOI: 10.1016/S1084-9521(02)00125-8]
9. Richardson MM, Jonsson JR, Powell EE, Brunt EM, Neuschwander-Tetri BA, Bhathal PS, Dixon JB, Weltman MD, Tilg H, Moschen AR, Purdie DM, Demetris AJ, Clouston AD. Progressive fibrosis in nonalcoholic steatohepatitis: Association with altered regeneration and a ductular reaction. *Gastroenterology* 2007; **133(1)**: 80-90. [PMID: 17631134]; [DOI: 10.1053/j.gastro.2007.05.012]
10. Nobili V, Carpino G, Alisi A, Franchitto A, Alpini G, Rita De Vito R, Onori P, Alvaro D, Gaudio E. Hepatic progenitor cells activation, fibrosis, and adipokines production in pediatric nonalcoholic fatty liver disease. *Hepatology* 2012; **56(6):** 2142-2153. [PMID: 22467277]; [DOI: 10.1002/hep.25742]
11. Libbrecht L, Desmet V, Van Damme B, Roskams T. Deep intralobular extension of human hepatic 'progenitor cells' correlates with parenchymal inflammation in chronic viral hepatitis: can 'progenitor cells' migrate? *J Pathol* 2000; **192 (3)**: 373-378. [PMID: 11054721]
12. Clouston AD, Powell EE, Walsh MJ, Richardson MM, Demetris AJ, Jonsson JR. Fibrosis correlates with a ductular reaction in hepatitis C: Roles of impaired replication, progenitor cells and steatosis. *Hepatology* 2005; **41(4):** 809-818. [PMID: 15793848]; [DOI: 10.1002/hep.20650]
13. Carpino G, Renzi A, Onori P, Gaudio E. Role of hepatic progenitor cells in nonalcoholic fatty liver disease development: cellular cross-talks and molecular networks. *Int J Mol Sci* 2013; **14(10):** 20112-20130. [PMID: 24113587]; [DOI: 10.3390/ijms141020112]
14. Roskams T, Yang SQ, Koteish A, Durnez A, DeVos R, Huang X, Achten R, Verslype C, Diehl AM. Oxidative stress and oval cell accumulation in mice and humans with alcoholic and nonalcoholic fatty liver disease. *Am J Pathol* 2003, **163 (4):**1301-1311. [PMID: 14507639]; [DOI: 10.1016/S0002-9440(10)63489-X]
15. Mak KM, Kwong AJ, Chu E, Hoo NM. Hepatic steatosis, fibrosis, and cancer in elderly cadavers. *Anat Rec* 2012; **295 (7):** 40-50. [PMID: 22139908]; [DOI: 10.1002/ar.21525]
16. Mak KM, Sehgal P, Harris CK. Factor VIII-related antigen (FVIIIRAg) detects phenotype change of sinusoidal to vascular endothelium in hepatic fibrosis of elderly cadavers. *International Scholarly Research Notices,* Volume 2014, Article ID839560, 10 pages. [PMID: 2743476]; [DOI: 10.1155/2014/839560]
17. Eleazar JA, Memeo L, Jhang JS, Mansukhani MM, Chin S, Park SM, Lefkowitch JH, Bhagat G. Progenitor cell expansion: an important source of hepatocyte regeneration in chronic hepatitis. *J Hepatol* 2004; **41(6):** 983-999. [PMID: 15582132]; [DOI: 10.1016/jhep.2004.08.017]
18. Delladetsima J, Alexandrou P, Giaslakiotis K, Psichogiou M, Hatzis G, Sypsa V, Dina Tiniakos D. Hepatic progenitor cells in chronic hepatitis C: A phenomenon of older age and advanced liver disease. *Virchows Arch* 2010; **457(4):** 457-466. [PMID: 20721577]; [DOI: 10.1007/s00428-010-0597-x]
19. Gadd VL, Skoien R, Powell EE, Fagan KJ, Winterford C, Horsfall L, Irvine K, Clouston AD. The portal inflammatory infiltrate and ductular reaction in human nonalcoholic fatty liver disease. *Hepatology* 2014; **59(4):**1393-1405, 2014. [PMID: 24254368]; [DOI: 10.1002/hep.26937]
20. Ren C, Paronetto F, Mak KM, Leo MA, Lieber CS. Cytokeratin 7 staining of hepatocytes predicts progression to more severe fibrosis in alcohol-fed baboons. *J Hepatol* 2003; **38 (6):**770-775. [PMID: 12763370]; [DOI: 10.1016/S0168-8278(03)00144-2]
21. Xiao, J-C, Jin X-L, Ruck P, Adam A, Kaiserling E. Hepatic progenitor cells in human liver cirrhosis: Immunohistochemical, electron microscopic and immunofluorescence confocal microscopic findings. *World J Gastroenterol.* 2004; **10(8)**: 1208-1211. [PMID: 15069727]; [DOI: 10.3748/wjg.v10.18.1208]
22. Dubuquoy L, Louvet A, Lassailly G, Truant S, Boleslawski E, Artru F, Maggiotto F, Gantier E, Buob D, Leteurtre E, Cannesson A, Dharancy S, Moreno C, Pruvot F-R, Bataller R, Mathurin P. Progenitor cell expansion and impaired hepatocyte regeneration in explanted livers from alcoholic hepatitis. *Gut* 2015; **64(12):**1949-1960. [PMID: 25731872]; [DOI: 10.1136/gutjnl-2014-308410]

23. Lanthier N, Rubbia-Brandt L, Lin-Marq N, Sophie Clément S, Jean-Louis Frossard J-L, Nicolas Goossens N, Hadengue A, Laurent Spahr L. Hepatic cell proliferation plays a pivotal role in the prognosis of alcoholic hepatitis. *J Hepatol* 2015; **63 (3):** 609-621. [PMID: 25872168]; [DOI: 10.1016/j.jhep.2015.04.003]
24. Sclair SN, Fiel MI, Wu H-S, Doucette J, Aloman C, Schiano TD. Increased hepatic progenitor cell response and ductular reaction in patients with severe recurrent HCV post-liver transplantation. *Clin Transplant* 2016; **30(6):**722-730. [PMID: 27027987]; [DOI: 10.111/ctr.12740]
25. Roskams T, Katoonizadeh A, Komuta M. Hepatic progenitor cells: An update. *Clin Liver Dis* 2010; 14:705-718. [PMID: 28506372]; [DOI: 10.1016/jcld.2010.08.003]
26. Yoon S-M, Gerasimidou D, Kuwahara R, Hytiroglou P, Yoo JE, Park YN, Theise ND. Epithelial cell adhesion molecule (EpCAM) marks hepatocytes newly derived from stem/progenitor cells in humans. *Hepatology* 2011; **53(3):** 964-973. [PMID: 21319194]; [DOI: 10.1002/hep.24122]
27. Sell S. Comparison of liver progenitor cells in human atypical ductular reactions with those seen in experimental models of liver injury. *Hepatology* 1998; **27(2):** 317-331. [PMID: 9462628]; [DOI: 10.1002/hep.510270202]
28. De Vos R, Desmet V. Ultrastructural characteristics of novel epithelial cell types in human pathological liver specimens with chronic ductular reaction. *Am J Pathol* 1992; **140(6):** 1441-1450. [PMID: 1605309]
29. Sancho-Bru P, Altamirano J, Rodrigo-Torres D, Coll M, Millán C, Lozano JJ, Miquel R, Arroyo V, Caballera J, Gines P. Bataller R. Liver progenitor cell markers correlate with liver damage and predict short-term mortality in patients with alcoholic hepatitis. *Hepatology* 2012; **55(6):** 1931-1941. [PMID: 22278680]; [DOI: 10.1002/hep.25614]
30. Williams MJ, Clouston AD, Forbes SJ. Links between hepatic fibrosis, ductular reaction, and progenitor cell expansion. *Gastroenterology* 2014; **146 (2):** 349-356. [PMID: 24315991]; [DOI: 10.1053/j.gastro.2013.11.034]

**Peer Reviewer:** Fethi Derbel